AMSE JOURNALS –2014-Series: Modelling B; Vol. 83; N° 1; pp 110-128

Submitted June 2014; Revised Dec. 26, 2014; Accepted Jan. 20, 2015

Effects of Hall Current and Viscous Dissipation on MHD Free Convection Fluid Flow in a Rotating System

*Abdul Quader, **Md. Mahmud Alam

Mathematics Discipline, Science, Engineering and Technology School, Khulna University
Khulna-9208, Bangladesh (*kafi0849@yahoo.com, **alam_mahmud2000@yahoo.com)

Abstract

The combined effects of Hall current and rotation on MHD unsteady free convective flow through a porous medium have been investigated. The uniform magnetic field and the suction velocity are applied perpendicular to the porous plate. The obtained non-dimensional, non-similar coupled non-linear and partial differential equations have been solved by explicit finite difference technique. Numerical solutions for velocities and temperature distributions are obtained for various parameters by the above-mentioned technique. The shear stresses and Nusselt number are also investigated. The stability conditions and convergence criteria of the explicit finite difference scheme are established for finding the restriction of the values of various parameters to get more accuracy. The obtained results are illustrated with the help of graphs to observe the effects of the Hall parameter (m) and magnetic parameter (M^2) along with various parameters.

Key words: MHD, Hall current, viscous dissipation, porous medium, finite difference

Nomenclature

x, y, z	Cartesian coordinates	κ	Thermal conductivity
u, v, w	Velocity components	μ_e	Magnetic permeability
υ	Coefficient of kinematic viscosity	ρ	Density of the fluid
m	Hall parameter	σ	Electrical conductivity
g	Gravitational acceleration	Ω	Angular velocity
C_p	Specific heat at constant pressure	k'	Porous medium permeability
β	Coefficient of thermal expansion	M^2	Magnetic parameter
H_0	Constant magnetic field	E_c	Eckert number
w_0	Constant suction velocity	P_r	Prandtl number

k	Permeability parameter	E_k	Ekman number
U	Dimensionless primary velocity	τ_x	Primary shear stress
V	Dimensionless secondary velocity	τ_y	Secondary shear stress
θ	Dimensionless temperature	N_u	Nusselt number

1. Introduction

MHD is the science of motion of electrically conducting fluid in presence of magnetic field. There are numerous examples of application of MHD principle. Engineers apply MHD principle in fusion reactors, dispersion of metals, metallurgy, design of MHD pumps, MHD generators and MHD flow meters etc. Magnetohydrodynamics is currently undergoing a period of great enlargement and differentiation of subject matter. The study of magnetohydrodynamics viscous flow with Hall current has important engineering applications like Hall accelerators, power generators, constructions of turbines and centrifugal machines. The MHD free convection with heat transfer in a rotating system has been studied due to its importance in astrophysics, geophysics, soil science, the underground water energy storage system and nuclear power reactors etc. The rotating flow of an electrically conducting fluid in presence of magnetic field has its importance in geophysical problems. The study of rotating flow problems is also important in the solar physics dealing with the sunspot development, the solar cycle and the structure of rotating magnetic stars. Considerable attention has been given to the unsteady free-convection flow of viscous incompressible and electrically conducting fluid in the presence of applied magnetic field in connection with the theory of fluid motion in the liquid core of the Earth, meteorological, and oceanographic applications. The study of magnetohydrodynamic viscous flows with Hall currents has important engineering applications like power generators and MHD accelerators. MHD in the present form is due to pioneer contribution of several notable authors like *Alfven* (1942) and *Cowling* (1957). It was emphasized by Cowling that when the strength of the applied magnetic field is sufficiently large, Ohm's law needs to be modified to include Hall current. In the presence of a strong magnetic field, the charged particles are tied to the lines of force, and this prevents their motion transverse to the magnetic field. Then, the tendency of the current to flow in a direction normal to both the electric and magnetic fields is called Hall effect and the corresponding current is known as Hall current. Further, it has been recognized that significant viscous dissipation may occur in natural convection in various devices which are subject to large decelerations or which operate at high rotative speeds. In addition, the

viscous dissipation effects may also be present in stronger gravitational fields e.g., on larger planets, in large masses of gas in space and in many geological processes.

In last few decades, the study of hydrodynamic and hydromagnetic boundary-layer flows with or without Hall current effects in a rotating fluid have received the attention of many research workers. *Batchelor* (1970) studied the boundary layer flow on a horizontal plate. The effect of uniform transverse magnetic field on such a layer was investigated by *Gupta* (1972). However, when the strength of the magnetic field is very strong, the effects of Hall current play a significant role in determining the flow features. On the other hand, the study of flow through porous medium has become of principal interest in many scientific and engineering applications. *Yamamoto and Iwamura* (1976) investigated the flow with convective acceleration through a porous medium. *Soundalkegar and Pop* (1979) studied the free convection flow past a vertical isothermal infinite porous plate in a rotating fluid. *Raptis et al.* (1981) extended the problem and have studied the effects of transverse magnetic field on hydromagnetic free convection considering Hall effects into account. *Raptis* (1983) discussed the unsteady free convective flow through a porous medium bounded an infinite vertical plate with constant suction. *Ram* (1990) investigated the effects of Hall current and wall temperature oscillation on convective flow in a rotating fluid through porous medium. *Takhar et al.* (2002) observed the MHD flow over a moving plate in a rotating fluid with magnetic field, Hall currents and free-stream velocity. *Haque and Alam* (2009) studied the transient heat and mass transfer by mixed convection flow from a vertical porous plate with induced magnetic field, constant heat and mass fluxes. *Ziaul Haque and Alam* (2011) investigated the micropolar fluid behaviours on unsteady MHD heat and mass transfer flow with constant heat and mass fluxes, joule heating and viscous dissipation. *Das and Jana* (2012) also studied the unsteady MHD free convection flow near a moving vertical plate in a porous medium. *Guchhait et al.* (2012) observed the combined effects of Hall currents and rotation on MHD mixed convection oscillating in a rotating vertical channel.

Hence, the purpose of the present study is to extend the work of *Guchhait et al.* (2012) and to investigate the effects of both Hall current and viscous dissipation of an electrically conducting fluid bounded by an infinite vertical porous plate in a rotating system. The proposed model has been transformed into non-similar coupled partial differential equation by usual transformations. The governing equations are solved numerically by using the explicit finite difference technique. Finally, the results of this study have been discussed graphically for different values of the well-known parameters.

2. Mathematical Analysis

An unsteady MHD free convective flow of an electrically conducting incompressible viscous fluid past an infinite vertical porous plate with the effects of Hall current is considered. Let the fluid rotate with uniform angular velocity Ω about the z-axis normal to the plate. It is assumed that there is a constant suction velocity. The flow is also assumed to be in the x-axis that is taken along the plate in the upward direction and z-axis is normal to it. At time $t > 0$, the temperature at the plate is constantly raised from T_w to T_∞ which is thereafter maintained constant. Where T_w and T_∞ are the temperatures at the wall and outside the plate respectively. A uniform magnetic field H_0 is imposed along the z-axis and the plate is taken to be electrically non-conducting. It is assumed that the induced magnetic field is negligible so that $\boldsymbol{H} = (0, 0, H_0)$. This assumption is justified when the magnetic Reynolds number is very small. The equation of conservation of electric charge $\nabla.\boldsymbol{J} = 0$ gives j_z = constant, where $\boldsymbol{J} = (j_x, j_y, j_z)$. This constant is assumed to be zero at the non conducting plate, therefore $j_z = 0$ everywhere in the flow. Since the plate is infinite in extent, all the physical variables except pressure depend on z and t only. Hence the equation of continuity $\nabla.\boldsymbol{q} = 0$ gives $w = -w_0 (> 0)$, where $q = (u, v, w)$. The generalized Ohm's law including the effect of Hall current (Cowling) is;

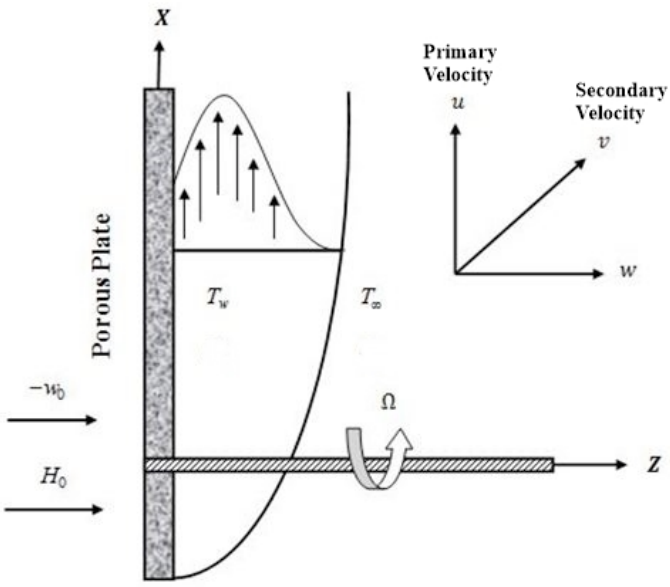

Fig. 1. Physical configuration and coordinate

$$\boldsymbol{J} + \frac{\omega_e \tau_e}{H_0}(\boldsymbol{J} \times \boldsymbol{H}) = \sigma\left(\boldsymbol{E} + \mu_e \boldsymbol{q} \times \boldsymbol{H} + \frac{1}{en_e}\nabla.p_e\right) \tag{1}$$

where ω_e is the cyclotron frequency and τ_e is electron collision time, σ is the electric conductivity, μ_e is the magnetic permeability, e is the electric charge, n_e is the number density of electron and p_e be the electron pressure. It has been assumed that the ion slip and thermoelectric effect is negligible. Further it is considered that the electric field $\boldsymbol{E} = 0$ and electron pressure have been neglected. Under this assumption equation (1) gives;

$$j_x = \frac{\sigma \mu_e H_0}{1+m^2}\left(v + mu\right) \tag{2}$$

$$j_y = \frac{\sigma \mu_e H_0}{1+m^2}\left(mv - u\right) \tag{3}$$

Thus, accordance with the above assumptions relevant to the problem and under the electromagnetic Boussinesq approximation, in a rotating frame the basic boundary layer equations are given by;

The momentum equations

$$\frac{\partial u}{\partial t} - w_0 \frac{\partial u}{\partial z} = \upsilon \frac{\partial^2 u}{\partial z^2} + g\beta\left(T - T_\infty\right) + 2\Omega v + \upsilon \frac{\sigma \mu_e {H_0}^2}{1+m^2}\left(mv - u\right) - \frac{\upsilon}{k'} u \tag{4}$$

$$\frac{\partial v}{\partial t} - w_0 \frac{\partial v}{\partial z} = \upsilon \frac{\partial^2 v}{\partial z^2} - 2\Omega u - \upsilon \frac{\sigma \mu_e {H_0}^2}{1+m^2}\left(v + mu\right) - \frac{\upsilon}{k'} v \tag{5}$$

The energy equation

$$\frac{\partial T}{\partial t} - w_0 \frac{\partial T}{\partial z} = \frac{\kappa}{\rho C_p}\frac{\partial^2 T}{\partial z^2} + \frac{\upsilon}{C_p}\left[\left(\frac{\partial v}{\partial z}\right)^2 + \left(\frac{\partial u}{\partial z}\right)^2\right] \tag{6}$$

with the corresponding boundary conditions are;

$$t > 0, \qquad u = w_0,\ v = 0,\ T = T_w \text{ at } z = 0 \tag{7}$$

$$u = 0,\ v = 0,\ T \to T_\infty \text{ as } z \to \infty \tag{8}$$

where u, v and w are the x, y and z components of velocity vector respectively, $m = \omega_e \tau_e$ is the Hall parameter, υ is the coefficient of kinematic viscosity, ρ is the density of the fluid, κ is thermal conductivity, C_p is the specific heat at constant pressure, g is the acceleration due to gravity, β is the coefficient of volume expansion and k' is the permeability of the porous medium. To obtain the governing equations and the boundary conditions in dimensionless form, the following non-dimensional quantities are introduced as;

$$Z = \frac{z w_0}{\upsilon}, U = \frac{u}{w_0}, V = \frac{v}{w_0}, \tau = \frac{t {w_0}^2}{\upsilon} \text{ and } \theta = \frac{T - T_\infty}{T_w - T_\infty}$$

Substituting the above relations in equations (4)-(6) and the boundary conditions (7) and (8) are;

$$\frac{\partial U}{\partial \tau} - \frac{\partial U}{\partial Z} = \frac{\partial^2 U}{\partial Z^2} + G_r \theta + 2E_k V + \frac{M^2}{1+m^2}\left(mV - U\right) - \frac{U}{k} \tag{9}$$

$$\frac{\partial V}{\partial \tau} - \frac{\partial V}{\partial Z} = \frac{\partial^2 V}{\partial Z^2} - 2E_k U - \frac{M^2}{1+m^2}\left(V + mU\right) - \frac{V}{k} \tag{10}$$

$$\frac{\partial \theta}{\partial \tau} - \frac{\partial \theta}{\partial Z} = \frac{1}{P_r}\frac{\partial^2 \theta}{\partial Z^2} + E_c\left[\left(\frac{\partial V}{\partial Z}\right)^2 + \left(\frac{\partial U}{\partial Z}\right)^2\right] \tag{11}$$

with the corresponding boundary conditions are;

$\tau > 0, \quad U = 1,\ V = 0,\ \theta = 1 \text{ at } Z = 0$ (12)

$U = 0,\ V = 0,\ \theta = 0 \text{ as } Z \to \infty$ (13)

where $G_r = \frac{\upsilon g \beta (T_w - T_\infty)}{w_0^3}$ (Grashof number), $E_k = \frac{\Omega \upsilon}{w_0^2}$ (Ekman number), $M^2 = \frac{\sigma \mu_e H_0^2 \upsilon}{\rho w_0^2}$ (Magnetic parameter), $k = \frac{w_0^2 k'}{\upsilon^2}$ (Permeability parameter), $E_c = \frac{w_0^2}{C_p (T_w - T_\infty)}$ (Eckert number), $P_r = \frac{\upsilon \rho C_p}{\kappa}$ (Prandtl number).

3. Shear Stresses and Nusselt Number

From the velocity field, the effects of various parameters on the plate shear stresses have been investigated. The primary shear stress is in the *x*-direction, $\tau_x = \mu \left(\frac{\partial u}{\partial z} \right)_{z=0}$ and the secondary shear stress is in the *y*-direction, $\tau_y = \mu \left(\frac{\partial v}{\partial z} \right)_{z=0}$ which are proportional to $\left(\frac{\partial U}{\partial Z} \right)_{Z=0}$ and $\left(\frac{\partial V}{\partial Z} \right)_{Z=0}$ respectively. From the temperature field, the effects of various parameters on heat transfer coefficient (Nusselt number) have been calculated. Nusselt number, $N_u = \mu \left(-\frac{\partial T}{\partial z} \right)_{z=0}$ which is proportional to $\left(-\frac{\partial \theta}{\partial Z} \right)_{Z=0}$. Here the details are not shown for brevity.

4. Numerical Technique

In this section, the governing second order coupled dimensionless partial differential equations with the associated initial and boundary conditions have been solved. For simplicity, the explicit finite difference method has been used to solve (9)-(11) correspond to the boundary conditions (12) and (13). The present problem requires a set of finite difference

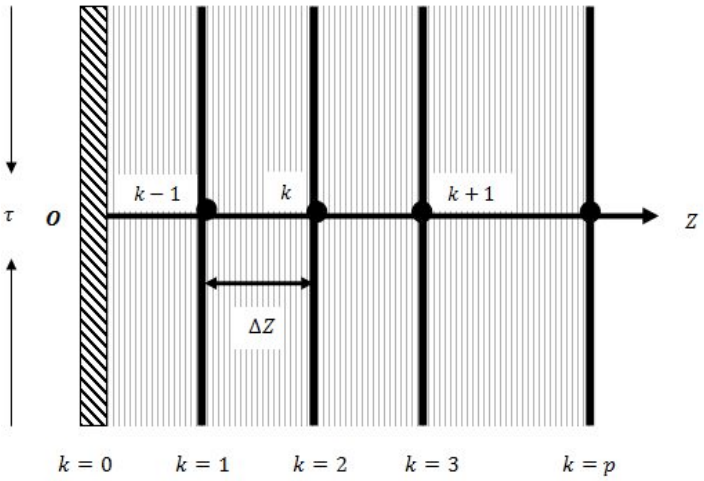

Fig. 2. Explicit finite difference system grid

equation. In this case the region within the boundary layer is divided by some perpendicular lines on Z-axis as shown in Fig. 2. It is assumed that the maximum length of boundary layer is $Z_{\max}(=25)$ as corresponds to $Z \to \infty$ i.e. Z varies from 0 to 25 and the number of grid spacing in Z direction is $p(=400)$, hence the constant mesh size along Z-axis becomes $\Delta Z = 0.0625(0 \le Z \le 25)$ with a smaller time space $\Delta\tau = 0.001$. Let U_k^{n+1}, V_k^{n+1} and θ_k^{n+1} denote values of U_k^n, V_k^n and θ_k^n at the end of time step respectively. The explicit finite difference approximation gives;

$$\frac{U_k^{n+1}-U_k^n}{\Delta\tau}-\frac{U_{k+1}^n-U_k^n}{\Delta Z}=\frac{U_{k+1}^n-2U_k^n+U_{k-1}^n}{(\Delta Z)^2}+G_r\theta_k^n+2E_kV_k^n+\frac{M^2}{1+m^2}\left(mV_k^n-U_k^n\right)-\frac{U_k^n}{k} \tag{14}$$

$$\frac{V_k^{n+1}-V_k^n}{\Delta\tau}-\frac{V_{k+1}^n-V_k^n}{\Delta Z}=\frac{V_{k+1}^n-2V_k^n+V_{k-1}^n}{(\Delta Z)^2}-2E_kU_k^n-\frac{M^2}{1+m^2}\left(V_k^n+mU_k^n\right)-\frac{V_k^n}{k} \tag{15}$$

$$\frac{\theta_k^{n+1}-\theta_k^n}{\Delta\tau}-\frac{\theta_{k+1}^n-\theta_k^n}{\Delta Z}=\frac{1}{P_r}\frac{\theta_{k+1}^n-2\theta_k^n+\theta_{k-1}^n}{(\Delta Z)^2}+E_c\left[\left(\frac{V_{k+1}^n-V_k^n}{\Delta Z}\right)^2+\left(\frac{U_{k+1}^n-U_k^n}{\Delta Z}\right)^2\right] \tag{16}$$

and the boundary conditions with the finite difference scheme are;

$$U_0^n=1,\ V_0^n=0,\ \theta_0^n=1 \tag{17}$$

$$U_L^n=0,\ V_L^n=0,\ \theta_L^n=0 \text{ where } L\to\infty \tag{18}$$

Here the subscript k designates the grid points with z coordinate and n represents a value of time, $\tau = n\Delta\tau$ where $n = 1,2,3,\ldots$. At the end of time step $\Delta\tau$, the new primary velocity U_k^{n+1}, the new secondary velocity V_k^{n+1} and the new temperature θ_k^{n+1} distributions at all interior nodal points, may be calculated by successive applications of (14) to (16) respectively. Also the numerical values of the shear stresses and Nusselt number are evaluated by Five-point approximate formula for their derivatives.

4. Stability and Convergence Analysis

Since an explicit procedure is being used, the analysis will remain incomplete unless the stability and convergence of the finite difference technique has been established. For the constant mesh sizes the stability criteria of the scheme may be established as follows. The general terms of the Fourier expansion for U_k^n, V_k^n and θ_k^n at a time arbitrarily called $\tau = 0$ are $e^{i\alpha Z}$ apart from a constant, where $i = \sqrt{-1}$. At a time τ later, these terms become;

$$U : \psi(\tau) e^{i\alpha Z}$$
$$V : \eta(\tau) e^{i\alpha Z} \tag{19}$$
$$\theta : \xi(\tau) e^{i\alpha Z}$$

and after the time step these terms become;

$$U : \psi'(\tau) e^{i\alpha Z}$$
$$V : \eta'(\tau) e^{i\alpha Z} \tag{20}$$
$$\theta : \xi'(\tau) e^{i\alpha Z}$$

Substituting (19) and (20) into (14) to (16), the following equations upon simplification have been obtained;

$$\frac{\psi'(\tau)-\psi(\tau)}{\Delta\tau} - \frac{\psi(\tau)\left(e^{i\alpha\Delta Z}-1\right)}{\Delta Z} = \frac{2\psi(\tau)\left(\cos\alpha\Delta Z-1\right)}{(\Delta Z)^2} + G_r\xi(\tau) + 2E_k\eta(\tau)$$
$$+\frac{M^2}{1+m^2}\left[m\ \eta(\tau)-\psi(\tau)\right] - \frac{\psi(\tau)}{k} \tag{21}$$

$$\frac{\eta'(\tau)-\eta(\tau)}{\Delta\tau} - \frac{\eta(\tau)\left(e^{i\alpha\Delta Z}-1\right)}{\Delta Z} = \frac{2\eta(\tau)\left(\cos\alpha\Delta Z-1\right)}{(\Delta Z)^2} - 2E_k\psi(\tau)$$
$$-\frac{M^2}{1+m^2}\left[\eta(\tau)+m\ \psi(\tau)\right] - \frac{\eta(\tau)}{k} \tag{22}$$

$$\frac{\xi'(\tau)-\xi(\tau)}{\Delta\tau} - \frac{\xi(\tau)\left(e^{i\alpha\Delta Z}-1\right)}{\Delta Z} = \frac{1}{P_r}\frac{2\xi(\tau)\left(\cos\alpha\Delta Z-1\right)}{(\Delta Z)^2}$$
$$+E_c\left[V\eta(\tau)\left(\frac{e^{i\alpha\Delta Z}-1}{\Delta Z}\right)^2 + U\psi(\tau)\left(\frac{e^{i\alpha\Delta Z}-1}{\Delta Z}\right)^2\right] \tag{23}$$

Equations (21), (22) and (23) can be written in the following form;

$$\psi' = A\psi + B\eta + C\xi$$
$$\eta' = -B\psi + A\eta \tag{24}$$
$$\xi' = D\psi + E\eta + F\xi$$

where, $A = 1 + \frac{\Delta\tau}{\Delta Z}\left(e^{i\alpha\Delta Z}-1\right) + \frac{2\Delta\tau}{(\Delta Z)^2}\left(\cos\alpha\Delta Z-1\right) - \frac{M^2}{1+m^2}\Delta\tau - \frac{\Delta\tau}{k}$

$$B = 2E_k\Delta\tau + m\frac{M^2}{1+m^2}\Delta\tau$$

$$C = G_r\Delta\tau$$

$$D = UE_c \frac{\Delta\tau}{(\Delta Z)^2}\left(e^{i\alpha\Delta Z} - 1\right)^2$$

$$E = VE_c \frac{\Delta\tau}{(\Delta Z)^2}\left(e^{i\alpha\Delta Z} - 1\right)^2$$

$$F = 1 + \frac{\Delta\tau}{\Delta Z}\left(e^{i\alpha\Delta Z} - 1\right) + \frac{1}{P_r}\frac{2\Delta\tau}{(\Delta Z)^2}\left(\cos\alpha\Delta Z - 1\right)$$

Equations (24) may be expressed in matrix form as follows;

$$\begin{bmatrix} \psi' \\ \eta' \\ \xi' \end{bmatrix} = \begin{bmatrix} A & B & C \\ -B & A & 0 \\ D & E & F \end{bmatrix} \begin{bmatrix} \psi \\ \eta \\ \xi \end{bmatrix}$$

That is $\varphi' = T\varphi$, where

$$\varphi' = \begin{bmatrix} \psi' \\ \eta' \\ \xi' \end{bmatrix}, T = \begin{bmatrix} A & B & C \\ -B & A & 0 \\ D & E & F \end{bmatrix} \text{ and } \varphi = \begin{bmatrix} \psi \\ \eta \\ \xi \end{bmatrix}$$

For obtaining the stability condition, it is necessary to find out eigenvalues of the amplification matrix T. For this explicit finite difference solution, the dimensionless time difference $\Delta\tau$ is very small that is tends to zero. Under this consideration, $B \to 0, C \to 0, D \to 0$ and $E \to 0$. For stability, the modulus of each eigenvalue of the amplification matrix T must not exceed unity.

Let, $a = \dfrac{\Delta\tau}{\Delta Z}, b = \dfrac{2\Delta\tau}{(\Delta Z)^2}, c = \Delta\tau$

Then, $A = 1 - 2\left[a + b + \left(\dfrac{M^2}{1+m^2} + \dfrac{1}{k}\right)\dfrac{c}{2}\right]$ and $F = 1 - 2\left[a + \dfrac{1}{P_r}b\right]$

Here, the coefficients a, b and c are real and non-negative. So, the maximum modulus of A and F occur when $\alpha\Delta Z = m\pi$. The values $|A|$ and $|F|$ are greater when m is odd integer. To satisfy $|A| \le 1, |F| \le 1$, the most negative allowable value are $A = -1$ and $F = -1$.

Hence, the stability conditions of the problem are as furnished below;

$$\frac{\Delta\tau}{\Delta Z} + \frac{2\Delta\tau}{(\Delta Z)^2} + \left(\frac{M^2}{1+m^2} + \frac{1}{k}\right)\frac{\Delta\tau}{2} \le 1 \text{ and } \frac{\Delta\tau}{\Delta Z} + \frac{1}{P_r}\frac{2\Delta\tau}{(\Delta Z)^2} \le 1 \tag{25}$$

Form the above equation (25) the convergence limits for the model of flow are $M^2 \le 443$, $m \ge 0.001$, $k \ge 0.002$ and $P_r \ge 0.5203$.

5. Results and Discussion

To investigate the practical situation of the problem, the numerical values of the dimensionless primary velocity (U), secondary velocity (V) and temperature (θ) within the boundary layer for the free convection flow have been obtained. Because of the great importance of cooling problem in nuclear engineering in connection with the cooling of reactors, the value of the Grashof number for heat transfer is taken positive. Since the most important fluids are atmospheric air, salt water and water so the results are limited to $P_r = 0.71$(Prandtl number for air at $20^o\mathrm{C}$), $P_r = 1.0$(Prandtl number for salt water at $20^o\mathrm{C}$) and $P_r = 7.0$ (Prandtl number for water at $20^o\mathrm{C}$). In addition, The values of Hall parameter (m), Magnetic parameter (M^2) and porous permeability parameter (k) are taken according to the convergence criteria. In this study, the values of other parameters E_k and E_c are chosen arbitrarily.

For steady state solutions of the problem, the computations have been carried out up to $\tau = 20$. It is observed that the values of this computation, however, show little changes after $\tau = 15$. Thus the solution at $\tau = 20$ are essentially steady-state solutions. The nature of primary velocity, secondary velocity, temperature distributions, shear stresses and Nusselt number are illustrated in Figs. 3-31 for different values of various parameters.

The primary velocity profile has a minor increasing effect for the rise of Hall parameter (m) which is presented in Fig. 3 while the secondary velocity decreases significantly with the increase of m in Fig. 4.

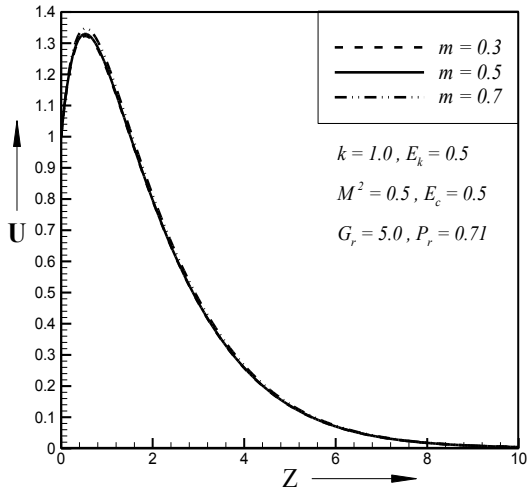

Fig. 3. Primary velocity profiles for different values of m

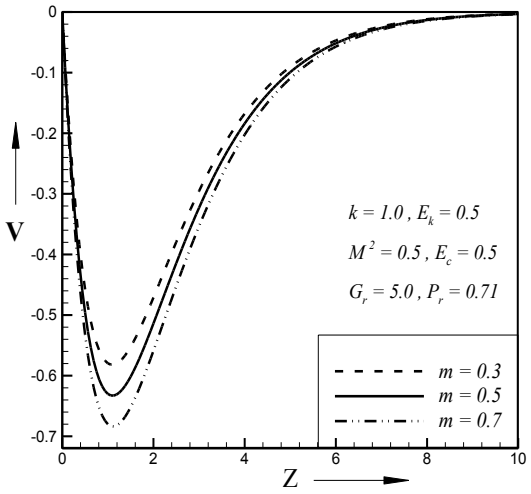

Fig. 4. Secondary velocity profiles for different values of m

It is analyzed that the primary velocity decreases with the rise of magnetic parameter (M^2) which is plotted in Fig. 5 while the secondary velocity shows the opposite nature of primary velocity for M^2 in Fig. 6. It has been shown in Fig. 7 that the increasing values of the Grashof number (G_r) increases the primary velocity profile while the secondary velocity profile shows reverse effect for G_r which is shown in Fig. 8.

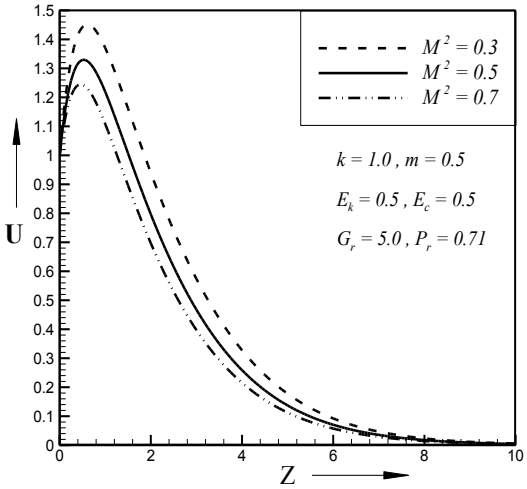

Fig. 5. Primary velocity profiles for different values of M^2

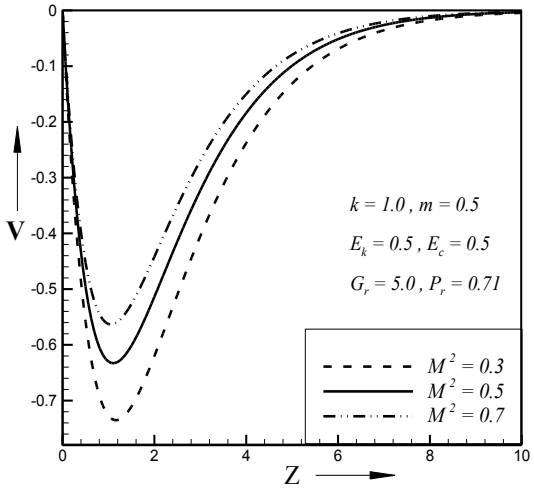

Fig. 6. Secondary velocity profiles for different values of M^2

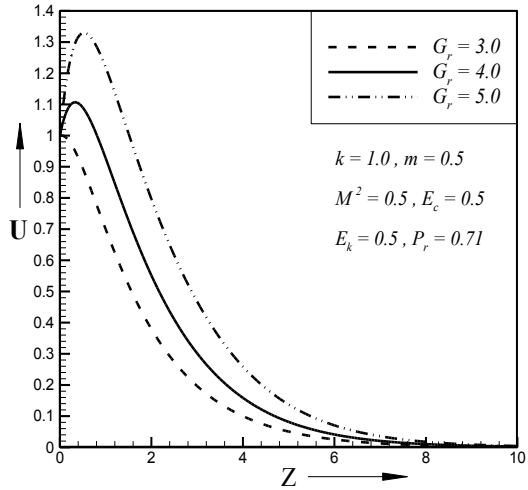

Fig. 7. Primary velocity profiles for different values of G_r

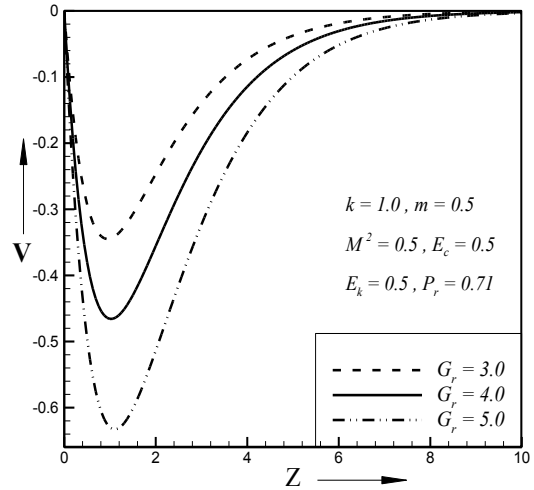

Fig. 8. Secondary velocity profiles for different values of G_r

It is observed in Fig. 9 and Fig. 10 that both the velocity profiles have a decreasing effect with the increase of Ekman number (E_k). In Fig. 11, the rise of porous permeability parameter (k) leads to an increase in primary velocity profiles while a decreasing effect on secondary velocity field is observed in Fig. 12 for increasing value of k.

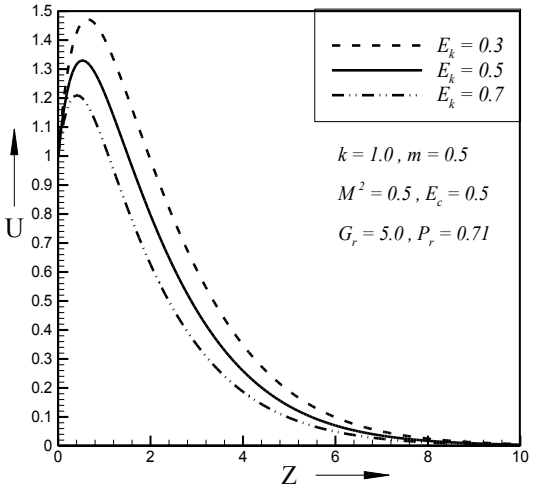

Fig. 9. Primary velocity profiles for different values of E_k

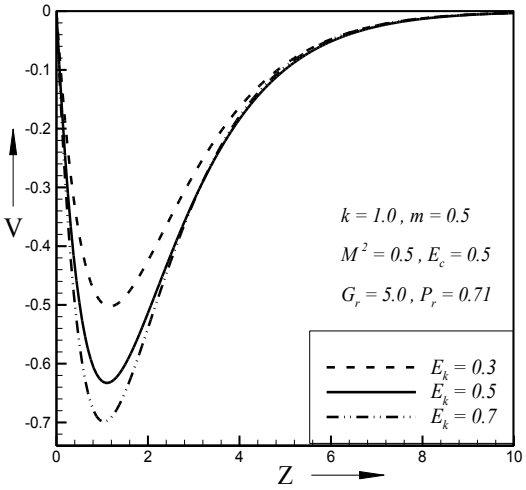

Fig. 10. Secondary velocity profiles for different values of E_k

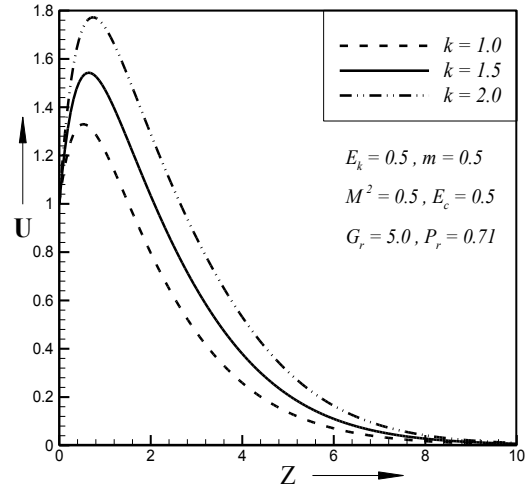

Fig. 11. Primary velocity profiles for different values of k

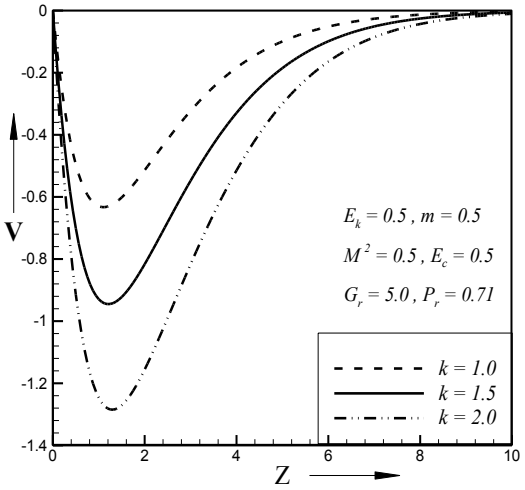

Fig. 12. Secondary velocity profiles for different values of k

The primary velocity increases with the increase of Eckert number (E_c) which has been observed in Fig. 13, while the secondary velocity decreases with the increase of Eckert number (E_c) which has been observed in Fig. 14. In Fig. 15, it has shown that the primary velocity profile decreases drastically for the increase of Prandtl number (P_r), while secondary velocity leads opposite nature of primary velocity profile for the increase of P_r which is shown in Fig. 16.

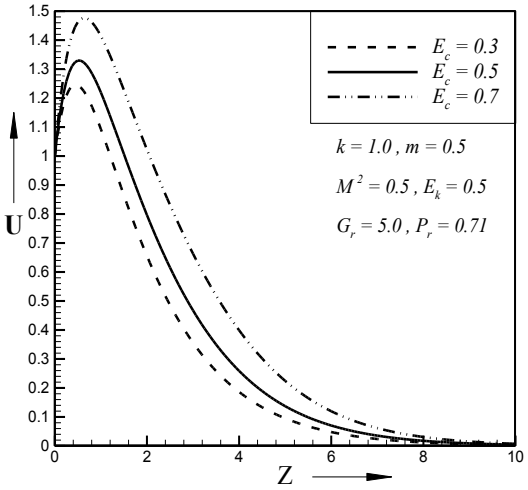

Fig. 13. Primary velocity profiles for different values of E_c

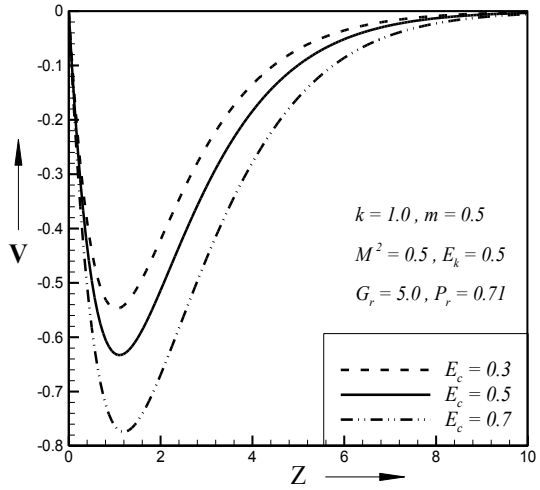

Fig. 14. Secondary velocity profiles for different values of E_c

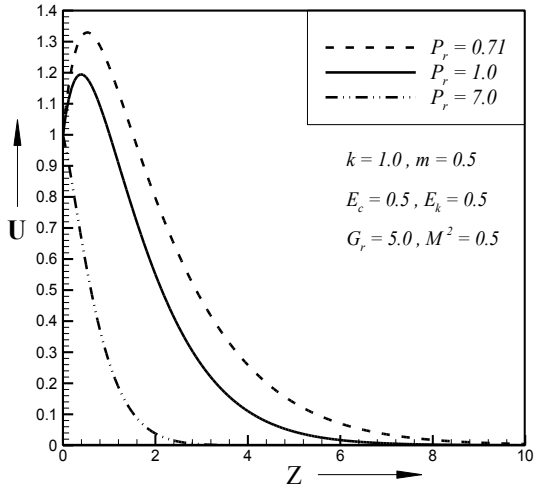

Fig. 15. Primary velocity profiles for different values of P_r

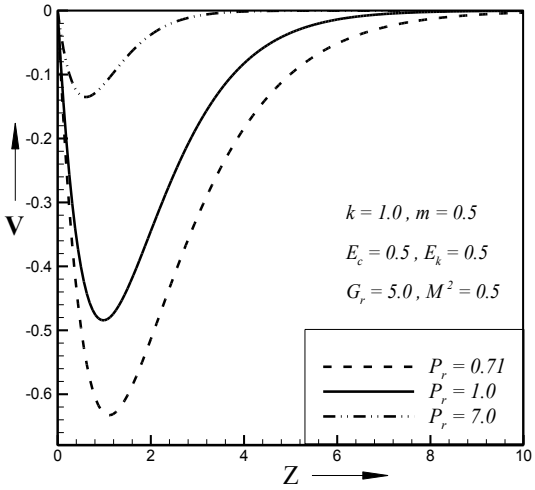

Fig. 16. Secondary velocity profiles for different values of P_r

Fig. 17 shows that there is a minor increasing effect on temperature distribution as Hall parameter (m) increases. The temperature decreases with the increase of Magnetic parameter (M^2), which is shown in Fig. 18. It is observed that temperature distribution has an increasing effect with the rise of G_r that is illustrated in Fig. 19. In Fig. 20, the rise of porous permeability parameter (k) leads to an increase in temperature distribution. From Fig. 21 it is shown that the increasing values of the Eckert number (E_c) increases the temperature distribution. The rise of Prandtl number (P_r) causes fall of temperature, that is shown in Fig. 22. The effect of Ekman number (E_k) on temperature (is not shown for brevity) follows the interesting pattern.

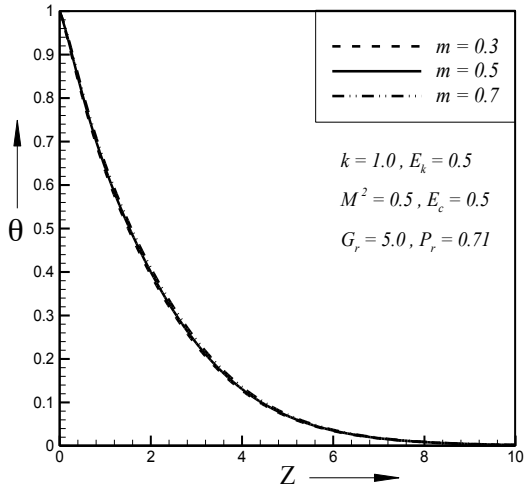

Fig. 17. Temperature profiles for different values of m

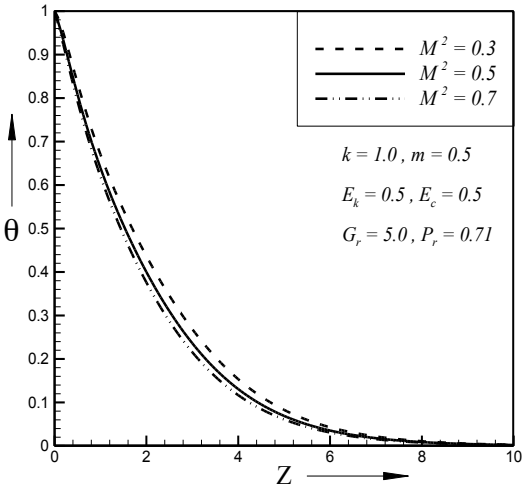

Fig.18. Temperature profiles for different values of M^2

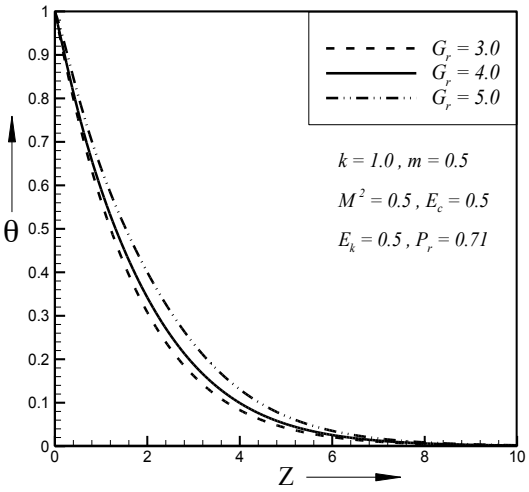

Fig. 19. Temperature profiles for different values of G_r

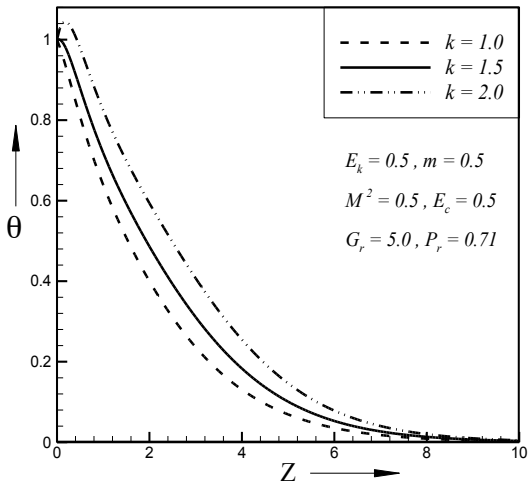

Fig.20. Temperature profiles for different values of k

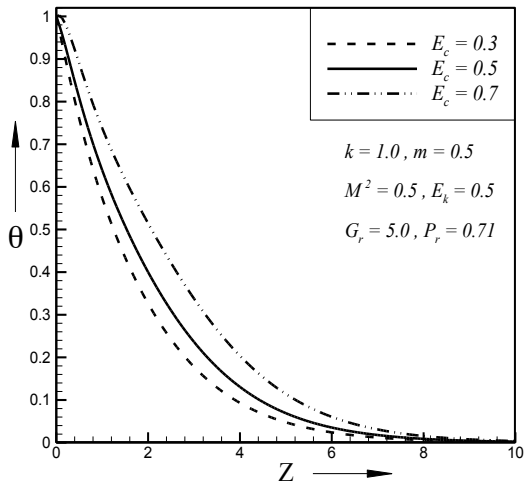

Fig. 21. Temperature profiles for different values of E_c

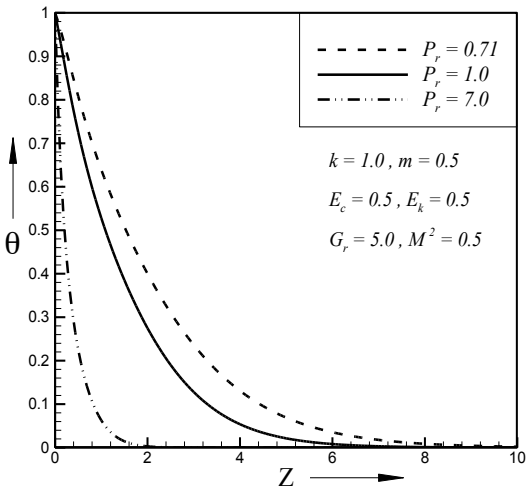

Fig.22. Temperature profiles for different values of P_r

In Fig. 23, it is observed that primary shear stress τ_x increases with the increase of both Hall parameter (m) and porous permeability parameter (k) whereas secondary shears stress τ_y decreases with the rise of both m and k that is shown in Fig. 24. Also, the primary shear stress τ_x decreases with the increase of Magnetic parameter (M^2) whereas it increases with the increase of Grashoff number (G_r), which are shown in Fig. 25. The secondary shear stress τ_y shows reverse effect of primary shear stress for M^2 and G_r as shown in Fig. 26. Primary shear stress τ_x increases with the rise of Eckert number (E_c) and decreases with the rise of Prandtl number (P_r) that is shown in Fig. 27 whereas secondary shears stress τ_y shows completely reverse effect for E_c and P_r that is shown in Fig. 28.

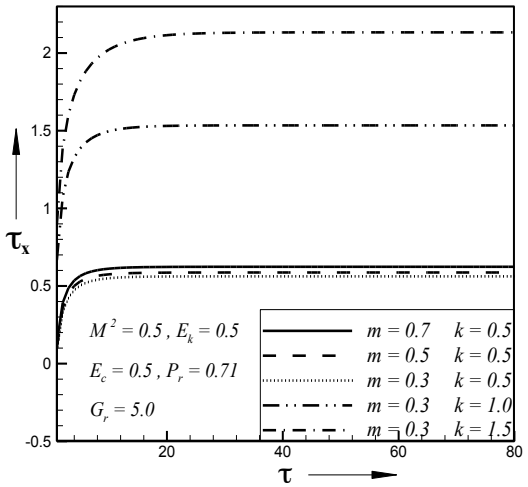

Fig. 23. Primary shear stress for different values of m and k

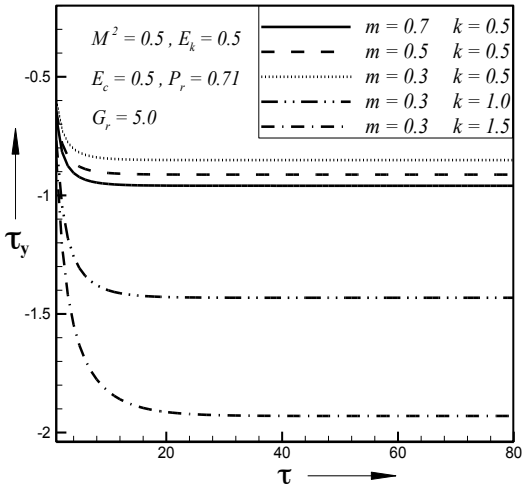

Fig. 24. Secondary shear stress for different values of m and k

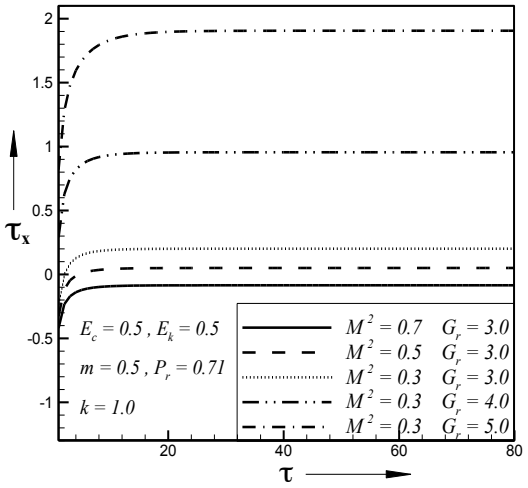

Fig. 25. Primary shear stress for different values of M^2 and G_r

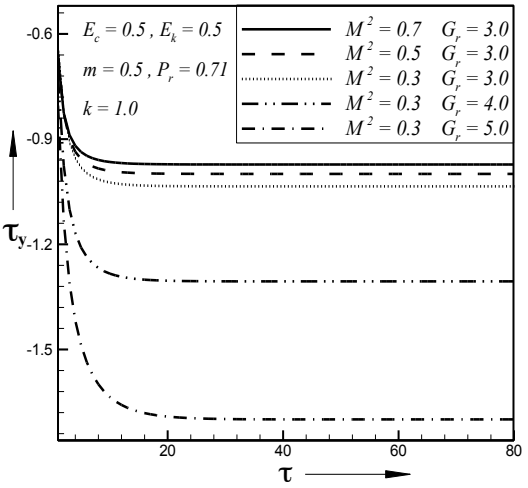

Fig. 26. Secondary shear stress for different values of M^2 and G_r

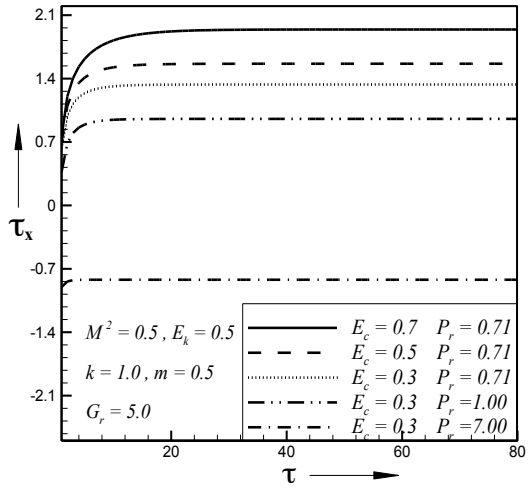

Fig. 27. Primary shear stress for different values of E_c and P_r

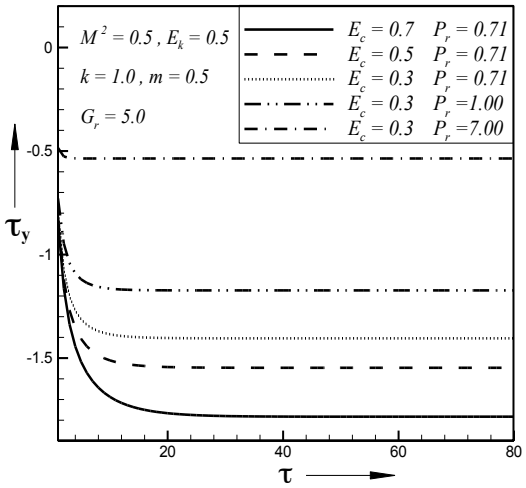

Fig. 28. Secondary shear stress for different values of E_c and P_r

The Fig. 29 shows that the Nusselt number has a minor increasing effect as Hall parameter (m) rises whereas it increases with the rise of porous permeability parameter (k). It is observed in Fig. 30 that the Nusselt number falls with the rise of Magnetic parameter (M^2) and increases with the increase of Grashoff number (G_r). In Fig. 31, the Nusselt number increases with the rise of E_c and decreases with the rise of P_r.

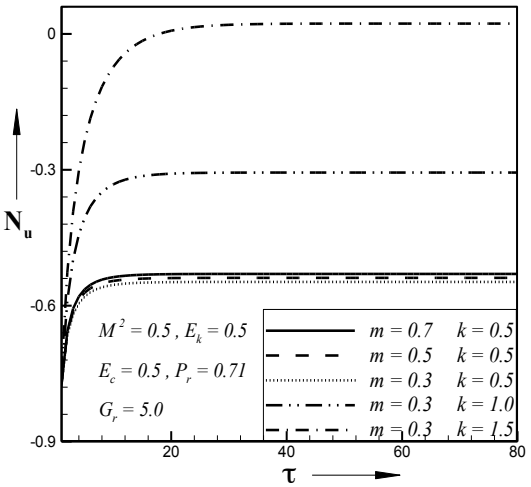

Fig. 29. Nusselt number for different values of m and k

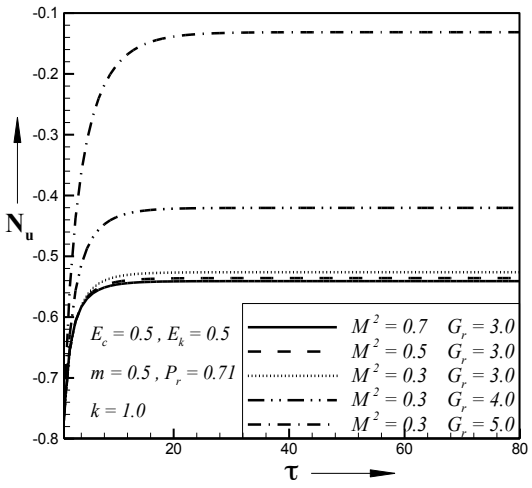

Fig. 30. Nusselt number for different values of M^2 and G_r

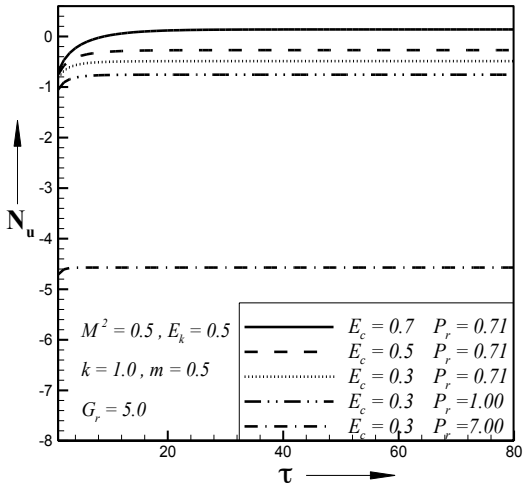

Fig. 31. Nusselt number for different values of E_c and P_r

Finally, a qualitative comparison of the present steady-state results with the published results of *Guchhait et al.* (2012) is presented in Table 1. The present results are qualitatively as well as quantitatively quite different in case of some flow parameters.

Increased Parameter	Previous results given by *Guchhait et al.* (2012)						Present results					
	U	V	θ	τ_x	τ_y	N_u	U	V	θ	τ_x	τ_y	N_u
m	Dec.	Inc.	N.E.	Dec.	Inc.	N.E.	Minor Inc.	Dec.	Minor Inc.	Inc.	Dec.	Minor Inc.
M^2	Dec.	Dec.		Dec.	Dec.		Dec.	Inc.		Dec.	Inc.	
G_r	Inc.	Inc.		Inc.	Inc.		Inc.	Dec.		Inc.	Dec.	
P_r	Inc.	Inc.	Inc.	Inc.	Inc.	Inc.	Dec.	Inc.	Dec.	Dec.	Inc.	Dec.
E_k	Dec.	Dec.		Dec.	Dec.		Dec.	Dec.		Dec.	Dec.	

Table 1. Qualitative comparison of the present results with previous results

6. Conclusions

In this study, the finite difference solution of unsteady MHD free convective fluid flow through a porous vertical plate in presence of Hall current and viscous dissipation in a rotating system is investigated. The obtained results are graphically presented for the variations of associated parameters. Some of the important findings of this observation are given below;

i. The primary velocity increases with the increase of m, k, G_r and E_c while it decreases with the increase of M^2, E_k and P_r.

ii. The secondary velocity increases with the increase of M^2 and P_r while it decreases with the increase of m, k, G_r, E_c and E_k.

iii. The fluid temperature is increasingly affected by k, G_r, E_c and E_k and decreasingly affected by M^2 and P_r.

iv. The primary shear stress increases with the increase of m, k, G_r and E_c while it decreases with the increase of M^2, E_k and P_r.

v. The secondary shear stress increases with the increase of M^2 and P_r while it decreases with the increase of m, k, G_r, E_c and E_k.

vi. The Nusselt number is increasingly affected by k, G_r, E_c and E_k and decreasingly affected by M^2 and P_r.

References

1. Alfven, H., "On the existence of electromagnetic Hydromagnetic waves", *Arkiv för Matematik, Astronomi Och Fysik,* Vol. 2, pp. 295, 1942.
2. Batchelor, G. K., "An Introduction to fluid Dynamics", *Cambridge University Press*, Cambridge, 1970.
3. Cowling, T. G., "Magnetohydrodynamics", *Interscience Publications,* New York, 1957.
4. Das, K. and Jana, S., "Heat and Mass transfer effects on unsteady MHD free convection flow near a moving vertical plate in a porous medium", *Bull. Soc. Math.*, Vol. 17, pp. 15-32, 2012.
5. Guchhait, S. K., Das, S. and Jana, R. N., "Combined effects of Hall currents and rotation on MHD mixed convection oscillating in a rotating vertical channel", *International Journal of Computer Applications*, Vol. 49, No. 13, pp. 1-11, 2012.
6. Gupta, A. S., "Magnetohydrodynamic Ekman layer", *Acta Mechanica*, vol. 13, pp. 155, 1972.
7. Haque, M. M. and Mahmud Alam, MD., "Transient heat and mass transfer by mixed convection flow from a vertical porous plate with induced magnetic field, constant heat and mass fluxes", *AMSE Journals*, Modelling, Measurement and Control, Mechanics and Thermics, Vol. 78, Nº 3/4, 2009 .
8. Ram, P. C., "Effects of Hall current and wall temperature oscillation on convective flow in a rotating fluid through porous medium", *Wärme-Stoffübertrag*, Vol. 25, pp. 205-208, 1990.

9. Raptis, A. A., Perdikis, C. P. and Tzivanidis, G.J., "Hydromagnetic free convection flow past a vertical infinite porous plate in a rotating fluid", *Acta Physica Academiae Scientiarum Hungaricae*, Vol. 50, pp. 373, 1981.
10. Raptis, A., "Unsteady free convective flow and mass transfer through a porous medium bounded by a infinite vertical limiting surface with constant suction and time-dependent temperature", *Journal of Energy Research*, Vol. 7, pp. 385-389, 1983.
11. Soundalgekar, V. M. and Pop, I., "Hydromagnetic free convection flow past a vertical infinite porous flat plate in a rotating fluid", *Acta Physica Academiae Scientiarum Hungaricae*, Vol. 47, pp. 313, 1979.
12. Takhar, H. S. , Chamkha, A. J. and Nath, G., "MHD flow over a moving plate in a rotating fluid with magnetic field, Hall currents and free-stream velocity", *International Journal of Engineering Science*, Vol. 40, pp. 1511-1527, 2002.
13. Yamamoto, K. and Iwamura, N., "Flow with convective acceleration through a porous medium", *Journal of Engineering Mathematics*, Vol. 10, pp. 41-54, 1976.
14. Ziaul Haque, Md. and Mahmud Alam, MD., "Micropolar fluid behaviours on unsteady MHD heat and Mass transfer flow with constant heat and mass fluxes, joule heating and viscous dissipation", *AMSE Journals*, Series 2B, Mechanics and Thermics, Vol. 80, Nº 1/2, 2011 .